XIV International Conference on Computational Plasticity. Fundamentals and Applications
COMPLAS XIV
E. Oñate, D.R.J. Owen, D. Peric & M. Chiumenti (Eds)

BIFURCATION ANALYSIS BASED ON A MATERIAL MODEL WITH STRESS–RATE DEPENDENCY AND NON–ASSOCIATED FLOW RULE FOR FRACTURE PREDICTION IN METAL FORMING

Tetsuo Oya*, Jun yanagimoto, Koichi Ito†, Gen Uemura† and Naomichi Mori†**

* Graduate School of Science and Technology, Keio University
3-14-1 Hiyoshi, Kohoku-ku, Yokohama, Japan
e-mail: oya@sd.keio.ac.jp

**Institute of Industrial Science, The University of Tokyo, Tokyo, Japan

†M &M Research Inc., Tokyo, Japan

Key words: Metal Forming, Fracture Prediction, Bifurcation Theory, Plastic Constitutive Equation, Stress–rate Dependency, Non–associated Flow Rule

Abstract. Recent increasing application of advanced high-strength metals causes growing demand for accurate fracture prediction in metal forming simulation. However, since the construction of objective and reliable fracture prediction method is generally difficult, essential progress in fundamental theory that supports evolution of fracture prediction framework is required.

In this study, a fracture prediction framework based on the bifurcation theory is presented. The main achievement is a novel material model based on stress-rate dependency related with non-associate flow rule. This model is based on non-associated flow rule with independent arbitrary higher-order yield function and plastic potential function for any anisotropic materials. And this formulation is combined with the stress-rate dependency plastic constitutive equation, which is known as Ito-Goya model, to construct a generalized plastic constitutive model in which non-normality and non-associativity are reasonably considered. Then, by adopting the three-dimensional bifurcation theory, which is known as the 3D localized bifurcation theory, more accurate prediction of the initiation of shear band is realized, leading to general and reliable construction of forming limit diagram. Then, by using virtual material data, numerical simulation is carried out to exhibit fracture limit diagram for demonstrating the generality and reliability of the proposed methodology. In particular, the effect of stress-rate dependency on the bifurcation analysis is investigated, and the order of the yield function is used to investigate the influence on the forming limit prediction.

1 INTRODUCTION

Recent increasing application of advanced high-strength metals causes growing demand for accurate fracture prediction in metal forming simulation. However, since the construction of objective and reliable fracture prediction method is generally difficult, essential progress in fundamental theory that supports evolution of fracture prediction framework is required. For example, many fracture prediction criteria have been proposed based on the concept of the ductile fracture model. This methodology uses criteria on the basis of physical observation by subjective or intuitive way. This is the reason why there are many criteria to predict the onset of fracture for various materials and forming types. However, the mechanism of the onset of fracture should be constructed free from material type and forming type to achieve accurate, physically reasonable and objective, and user-friendly fracture prediction framework. To realize this aim, because fracture is a terminal phenomena happens at the end of large plastic deformation, the authors considered that reliable and useful fracture prediction scheme should be invented faithfully based on the theory of plasticity.

For constructing reliable fracture prediction model, the bifurcation theory has been adopted in this research, and a novel material model to conduct bifurcation analysis was developed. Although the onset of localized bifurcation is not equivalent to the rapture of a material, this phenomena is closely related with material fracture particularly in sheet metal. Therefore, building an analytical methodology for fracture prediction based on the bifurcation theory is meaningful. The bifurcation theory as a fracture prediction method is advantageous in terms of generality and objectivity, but it is known that the bifurcation analysis using conventional material models sometimes exhibit poor result. General bifurcation theory was established by Hill [1] for plastic materials, followed by many researches based on it. These were based on plane-stress condition and on normality rule; under these assumptions, accurate prediction of the initiation of shear band, which is considered as a sign of fracture, is almost impossible. Even with the S-R (Stören-Rice) theory [2] in which stress-rate dependency is considered, there is still a restriction of plane-stress condition. Thus, to conduct bifurcation analysis appropriately, a new framework that can deal with three-dimensional bifurcation mode and abrupt change in stress field should be created.

In this study, a material model based on stress-rate dependency related with non-associate flow rule is presented. This model is based on non-associated flow rule with arbitrary higher order yield function and plastic potential function for any anisotropic materials [3][4]. And this formulation is combined with the stress-rate-dependency plastic constitutive equation, which is known as the Ito-Goya plastic constitutive equation [5], to construct a generalized plastic constitutive model in which non-normality and non-associativity can be reasonably included. Then, by adopting the three-dimensional bifurcation theory [5], more accurate prediction of the initiation of shear band is realized, leading to general and reliable construction of forming limit diagram.

In this paper, the above-mentioned theoretical framework is described. Then, by using virtual material data, numerical simulation is carried out to exhibit fracture limit diagram

for demonstrating the effectiveness of the proposed methodology.

2 PROPOSED MODEL AND FRAMEWORK FOR FRACTURE PREDICTION

2.1 Material model

First, the material model proposed by the authors[3][4], which plays an essence role in this research, is described. This model is constructed to express deformation anisotropy and yield stress anisotropy by using non-associated flow rule formulation with the number of material constants same as that of Hill's 1948 model. The following is the definition of the yield function and the plastic potential function and the equivalent plastic strain increment.

In the proposed model, we defined the yield function $f(\boldsymbol{\sigma})$ as being equal to the equivalent stress; namely, the expression is

$$f(\boldsymbol{\sigma}) = \bar{\sigma} = \sqrt[2m_y]{\frac{3}{2(F+G+H)}\left(\boldsymbol{s}_{m_y}\cdot\boldsymbol{A}\cdot\boldsymbol{s}_{m_y}\right)}. \tag{1}$$

Here, the matrix $\boldsymbol{A}$ has the anisotropic parameters in its diagonal terms; and the pseudo-vector $\boldsymbol{s}_{m_y}$ is a set of deviatoric stress components to the power of m_y. This higher-order function preserves the form of Hill's quadratic yield function, that is, it contains the same anisotropic parameters F, G, H, L, M, and N. This feature is important because it is possible to construct a higher-order yield function by changing the power value m_y without increasing the number of undetermined variables.

In our non-associated flow rule-based formulation, a function different from the yield function is adopted as a plastic potential function, which provides the direction of the plastic strain increment of the subsequent state of current stress. In this study, the previously introduced function $f(\boldsymbol{\sigma})$ is used as the yield function, and another function $g(\boldsymbol{\sigma})$ that takes the same form as $f(\boldsymbol{\sigma})$ but has different anisotropic parameters F^*, G^*, H^*, L^*, M^*, and N^* is adopted as the plastic potential function. In this expression, asterisks are used to distinguish $f(\boldsymbol{\sigma})$ from $g(\boldsymbol{\sigma})$. For example, the anisotropy matrix $\boldsymbol{A}$ is changed to $\boldsymbol{A}^*$, in which the original parameters F, G, H, L, M, and N are also changed to F^*, G^*, H^*, L^*, M^*, and N^*, respectively. To express another order of the function, the power variable m_p is used instead of m_y. Thus, the plastic potential function of the proposed model takes the form of

$$g(\boldsymbol{\sigma}) = \bar{\sigma}^* = \sqrt[2m_p]{\frac{3}{2(F^*+G^*+H^*)}\left(\boldsymbol{s}_{m_p}\cdot\boldsymbol{A}^*\cdot\boldsymbol{s}_{m_p}\right)}. \tag{2}$$

From the definition of the plastic work, an explicit expression for the equivalent plastic strain increment is obtained as

$$d\bar{\varepsilon}^p = \frac{m_p\overline{\sigma}^{*m_p}}{\overline{\sigma}}\sqrt{\frac{2(F^*+G^*+H^*)}{3}\left(\boldsymbol{D}'^*_{m_p}\cdot d\boldsymbol{e}^p\right)^T\cdot\left\{\boldsymbol{A}^*\cdot\left(\boldsymbol{D}'^*_{m_p}\cdot d\boldsymbol{e}^p\right)\right\}}. \tag{3}$$

The main disadvantage of the non-associated flow rule models would be the increase in the number of unknown variables. Usually, these variables can be specified from experiments such as tensile tests; therefore, the use of the non-associated flow rule model could lead to an increased burden of experiments and measurements. In addition, if a higher-order function is required, the burden increases, making this approach impractical. Thus, to enjoy the benefits of the non-associated flow rule model, an increase in the numbers of unknown variables should be avoided, and this demand is considerably achieved with the proposed model.

The plastic anisotropy characteristics of materials are classified into two categories; namely, plastic flow stress anisotropy and plastic deformation anisotropy. The former and latter should be incorporated in the yield function and the plastic potential function, respectively. Consider cold-rolled metal sheets under a plane stress state. Under the plane stress condition, the number of variables is halved. The anisotropic variables that must be determined are F, G, H, and N and F^*, G^*, H^*, and N^*. The former set expresses the yield stress anisotropy and the latter set expresses the deformation anisotropy.

The parameters about stress anisotropy, F, G, and H, are determined by the yield stresses that are obtained by tensile test in rolling direction, transverse direction, and equibiaxial test. The parameters about deformation anisotropy, F^*, G^*, H^*, and N^*, are determined by the r-values in the direction of rolling, diagonal, and transverse. The remaining parameter N is determined by optimization using the tensile test data in the diagonal direction. Note that the diagonal yield stress, usually denoted as σ_{45}, is not used because the directions except for the rolling and transverse directions are not anisotropic principal axis and it is difficult to separate with the shear component. The order of the functions, m_y and m_p, should be determined before these anisotropic parameters are determined because these values specify the function type, and have own physical meaning different from the anisotropic parameters.

2.2 Ito-Goya's plastic constitutive model

Local bifurcation brings abrupt change on the current strain rate direction. Since the classical J_2 theory does not allow the rotation of the strain rate direction caused by the subsequent stress rate direction, it is not appropriate to the bifurcation problems. Therefore, in this study, Ito-Goya's plastic constitutive equation [5] is applied, because this model can take the dependency of the strain rate direction on the stress rate direction into account. Ito-Goya's plastic constitutive equation is represented as

$$d\boldsymbol{\varepsilon}^p = \Lambda \left(\boldsymbol{n}_F : \boldsymbol{l}_p \right) |d\boldsymbol{\sigma}'| \left[K_C \boldsymbol{l} + (1 - K_C) \boldsymbol{n}_N \right], \tag{4}$$

where $\boldsymbol{n}_N$ is an unit tensor called natural direction. This tensor indicates the direction of the deviatoric stress rate that is identical to that of the plastic strain rate. The unit tensor $\boldsymbol{n}_F$ is the direction of the gradient of the yield function and $\boldsymbol{l}$ is the direction of current deviatoric stress. In Eq. (4), the parameter K_C, which takes a value between 0 and 1, shows the dependency of the direction of the strain rate on stress rate. When K_C is equal to 1, the Ito-Goya's constitutive equation becomes the J_2 flow theory.

2.3 3D local bifurcation theory

Based on Hill's general bifurcation theory, bifurcation occurs at when the following condition is satisfied.

$$I[\Delta \boldsymbol{v}] = \int \Delta \boldsymbol{L} : \Delta \dot{\boldsymbol{S}} dV = 0, \tag{5}$$

where $\Delta \boldsymbol{v}$ is velocity field, $\boldsymbol{L}$ and $\dot{\boldsymbol{S}}$ are velocity gradient tensor and 1st Piola-Kichhoff stress tensor rate, respectively. $\dot{\boldsymbol{S}}$ can be represented by the Cauchy stress tensor as

$$\dot{\boldsymbol{S}} = \boldsymbol{D} : \dot{\varepsilon} + \boldsymbol{\omega} \cdot \boldsymbol{\sigma} - \boldsymbol{\sigma} \cdot \boldsymbol{\omega} - \boldsymbol{L} \cdot \boldsymbol{\sigma} = \boldsymbol{A} : \boldsymbol{L}, \tag{6}$$

where $\dot{\boldsymbol{\varepsilon}}$, $\boldsymbol{\omega}$, $\boldsymbol{D}$ are strain rate tensor, spin tensor, and tangent stiffness tensor, respectively. And $\boldsymbol{A}$ is a fourth rank tensor that relates the nominal stress rate and velocity gradient tensor $\boldsymbol{L}$. To characterize the bifurcation mode, the velocity gradient tensor is allowed to be discontinuous when the velocity gradient tensor crosses the bifurcation border Γ. $\boldsymbol{L}$ can be represented by the normal vector $\boldsymbol{n}$ on the bifurcation border and the local deformation mode vector $\boldsymbol{m}$ that is normal to $\boldsymbol{n}$ as

$$\boldsymbol{L} = \boldsymbol{m} \otimes \boldsymbol{n}. \tag{7}$$

The mode vector $\boldsymbol{m}$ can be composed of two different vectors in the Γ plane; namely, $\boldsymbol{m}_{\mathrm{SH}}$ and $\boldsymbol{m}_{\mathrm{SV}}$ are the vectors in horizontal and vertical direction, respectively. These vectors are expressed with three angle parameters; ϕ, ψ and θ, as shown in Fig.1. Specific expressions for these vectors are as follows.

$$\boldsymbol{n} = (\sin\phi\cos\psi,\ \sin\phi\sin\psi,\ \cos\phi)\,, \tag{8}$$
$$\boldsymbol{m}_{\mathrm{SH}} = (-\sin\phi,\ \cos\psi,\ 0)\,, \tag{9}$$
$$\boldsymbol{m}_{\mathrm{SV}} = (\cos\phi\cos\psi,\ \cos\phi\sin\psi,\ -\sin\phi)\,, \tag{10}$$
$$\boldsymbol{m} = \boldsymbol{m}_{\mathrm{SH}}\cos\theta + \boldsymbol{m}_{\mathrm{SV}}\sin\theta. \tag{11}$$

Substituting Eq. (6) and (7) into (5), we have the following bifurcation criterion

$$I[\boldsymbol{m}, \boldsymbol{n}; \boldsymbol{\sigma}] = hH[\boldsymbol{m}, \boldsymbol{n}; \boldsymbol{\alpha}] - \sigma\Sigma[\boldsymbol{m}, \boldsymbol{n}; \boldsymbol{\alpha}], \tag{12}$$

where the first and second term of this functional are described as

$$H[\boldsymbol{m}, \boldsymbol{n}; \boldsymbol{\alpha}] = \boldsymbol{m} \cdot \boldsymbol{n} \cdot \overline{\boldsymbol{D}}(\boldsymbol{s}) \cdot \boldsymbol{n} \cdot \boldsymbol{m}, \quad \text{where} \quad \overline{\boldsymbol{D}}(\boldsymbol{s}) \equiv \boldsymbol{D}(\boldsymbol{s})/h, \tag{13}$$
$$\Sigma[\boldsymbol{m}, \boldsymbol{n}; \boldsymbol{\alpha}] = \frac{1}{2}\left[\boldsymbol{m} \cdot \boldsymbol{\alpha} \cdot \boldsymbol{m} - \boldsymbol{n} \cdot \boldsymbol{\alpha} \cdot \boldsymbol{n}\right]. \tag{14}$$

In an elasto-plastic material subjected to large strain, ignoring elastic deformation, the tangent stiffness tensor can be assumed to be proportional to the hardening rate h.

Then, the current stress is represented by

$$\boldsymbol{\sigma} = \sigma\boldsymbol{\alpha}, \quad \sigma = \sqrt{\boldsymbol{\sigma} : \boldsymbol{\sigma}}, \quad \boldsymbol{\alpha} = \boldsymbol{\sigma}/\sigma, \tag{15}$$

where σ and $\boldsymbol{\alpha}$ are the norm of the current stress tensor and normalization tensor which gives stress ratios for each stress component, respectively.

Based on these relations, finally have the following local bifurcation criterion.

$$\left(\frac{\sigma}{h}\right)_{\mathrm{cr}} = \min\left(\frac{H[\boldsymbol{m},\boldsymbol{n};\boldsymbol{\alpha}]}{\Sigma[\boldsymbol{m},\boldsymbol{n};\boldsymbol{\alpha}]}\right). \tag{16}$$

The bifurcation criterion represented by Eq.(16) indicates that the local bifurcation, which is specified by the mode vectors $\boldsymbol{m}$ and $\boldsymbol{n}$ that are based on the current stress ratio tensor $\boldsymbol{\alpha}$, should be identified by the ratio σ/h that means the ratio of the stress level to the work-hardening. Mechanically, stress σ means the intensity of fracture initiation, and the hardening coefficient h means the material's resistance against fracture. Therefore, the formability represented in the σ/h plane is free from the strain-path-dependency that is usually observed in a typical FLD (Forming Limit Diagram) represented in strain space. Thus, because exhibiting forming limits on the σ/h plane is mechanically reasonable, this new expression is called SHFLD.

The fracture limits in the SHFLD can show 3D local bifurcation limits. The probable fracture would be lie between the lower bound represented by the S-R limit and the upper bound represented by the 3D local bifurcation limit.

3 BIFURCATION ANALYSIS

By using the theoretical framework described in the previous section, numerical analyses have been conducted to investigate the characteristics of the proposed method. In this analysis, assuming plane-stress condition, an isotropic material was considered with the following constants; $F = G = H = F^* = G^* = H^* = 1$, $L = M = N = L^* = M^* = N^* = 3$, Young ' s modulus = 210 GPa, Poisson ' s ratio $\nu = 0.3$, $n = 0.2$ and $K = 5.0 \times 10^8$ in the n-power law for material hardening. The order of the yield function and the plastic potential function, m_y and m_p, were set to 1. Parameters used in this investigation were the K_C value in the Ito-Goya model, and a strain value ε_h which determines the evaluation point of work-hardening coefficient included in the parameter Λ in Equation (4). In the construction of the tangent stiffness tensor in Equation (13), the component of the original tensor $\boldsymbol{D}$ was assumed linear in terms of hardening coefficient h; however, the tensor $\boldsymbol{D}$ is not actually linear with h. In this study, instead of dealing with the tensor $\boldsymbol{D}$ as nonlinear one, we assumed this as a linear tensor as for the hardening h for computational simplicity and investigated the effect of the hardening term on the analysis.

Bifurcation analyses were conducted as follows. The minimum value of the functional represented in the right-hand-side of Equation (16) was searched by changing the variables included in the fracture mode vectors, $\boldsymbol{m}$ and $\boldsymbol{n}$. The simulated annealing algorithm was adopted in this optimization process. To calculate the yield function in the used equations, a stress ratio α was used to control the stress condition; for example, $\alpha = 0$ for uniaxial, $\alpha = 1$ for equi-biaxial stress condition. The obtained minimum values were used to show the bifurcation initiation as the possible fracture onset in the fracture limit diagram exhibited in the σ/h plane, as shown in the following figures.

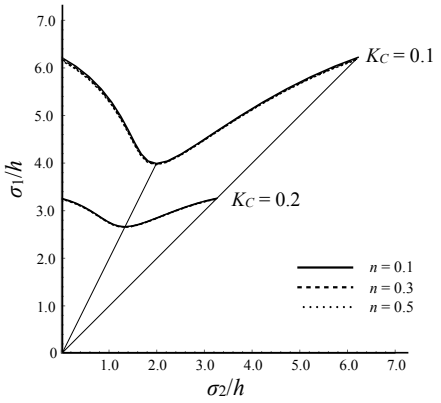

Figure 1: SHFLD for different n values.

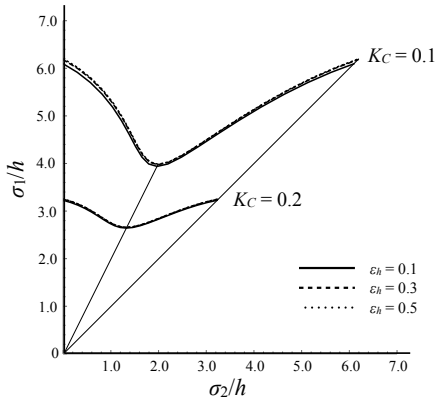

Figure 2: SHFLD for different work-hardening evaluation point ε_h.

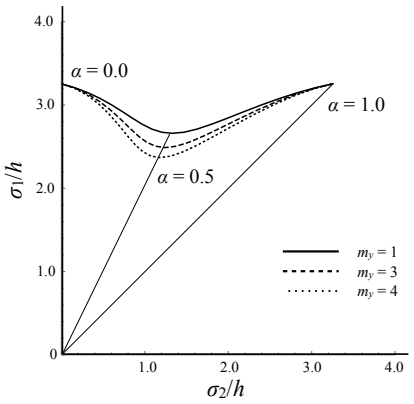

Figure 3: SHFLD for different m_y values.

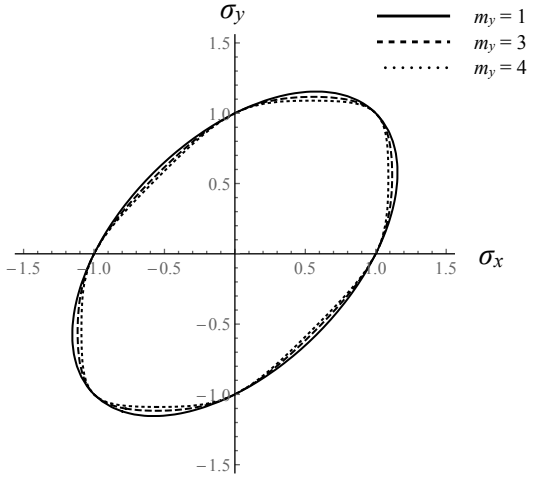

Figure 4: Yield surfaces for different m_y values.

In Figure 1, the effect of the n value on the fracture limit curve is shown. And in Figure 2, the effect of the work-hardening evaluation strain ε_h on the fracture limit curve is shown. In both figures, there are two sets of curves that are calculated with different K_C values (0.1 and 0.2). From these figures, as a apparent tendency, work-hardening properties do not affect the shape of curves and the only parameter that changes the curve is K_C value. In other words, the fracture limit curve exhibited on the SHFLD is almost independent from the material's hardening characteristics. This means the predicted limit is free from the strain path. Furthermore, this results support our assumption that the hardening property does not affect the minimum search and show that the linearization procedure explained above is valid. Then, the influence of the K_C value on fracture prediction is confirmed. Generally, as the K_C value increases, fracture limit deteriorates because of the growing stress-rate dependency. As seen in these figures, the fracture limit lines descend with the increased K_C value. This means the conducted bifurcation analyses were valid and shows physically reasonable tendency.

In Figure 3, the effect of the order of the yield surface on the limit curve is investigated. Since setting $m_y = 2$ brings same result with $m_y = 1$, the parameter m_y is varied as 1, 3 and 4. Clear descent of the curves can be observed around the plane-strain situation ($\alpha = 0.5$), on the other hand, no difference can be seen at tensile ($\alpha = 0$) and equi-biaxial ($\alpha = 1.0$) conditions. This result is quite reasonable because the stress level drops at the plane-strain condition, as shown in Figure 4, in the case of higher order yield function.

4 CONCLUSION

This paper has described the proposed fracture prediction framework that consists of the anisotropic material model based on non-associated flow rule, the Ito-Goya ' s stress-rate dependent constitutive equation, and the 3D bifurcation theory. And a new concept of fracture limit exhibition, which is called SHFLD, has been introduced. Numerical investigations have been carried out with virtual material data to show the effectiveness of the proposed method. Physically reasonable results were obtained from these analyses and the authors have confirmed that the assumptions made in this study is valid. There are many possible situations that have not tested yet; therefore, more numerical exploration and mechanical considerations would be conducted.

REFERENCES

[1] Hill, R., *J. Mech. Phys. Solids*, **7**, 209, (1959).

[2] Stören, S. and Rice, J. R., *J. Mech. Phys. Solids*, **23**, 421, (1975).

[3] Oya, T., Yanagimoto, J., Ito, K., Uemura, G. and Mori, N., *Procedia Engineering*, **81**, 1210, (2014).

[4] Oya, T., Yanagimoto, J., Ito, K., Uemura, G. and Mori, N., *MATEC Web of Conferences*, **80**, 05003, (2016).

[5] Ito, K., Sato, K., Goya, M. and Yoshida, T., *Int. J. Mech. Sci*, **42**, 2233, (2000).